RESEARCH ARTICLE

Figures and figure supplements

Signaling diversity enabled by Rap1-regulated plasma membrane ERK with distinct temporal dynamics

Jeremiah Keyes *et al*

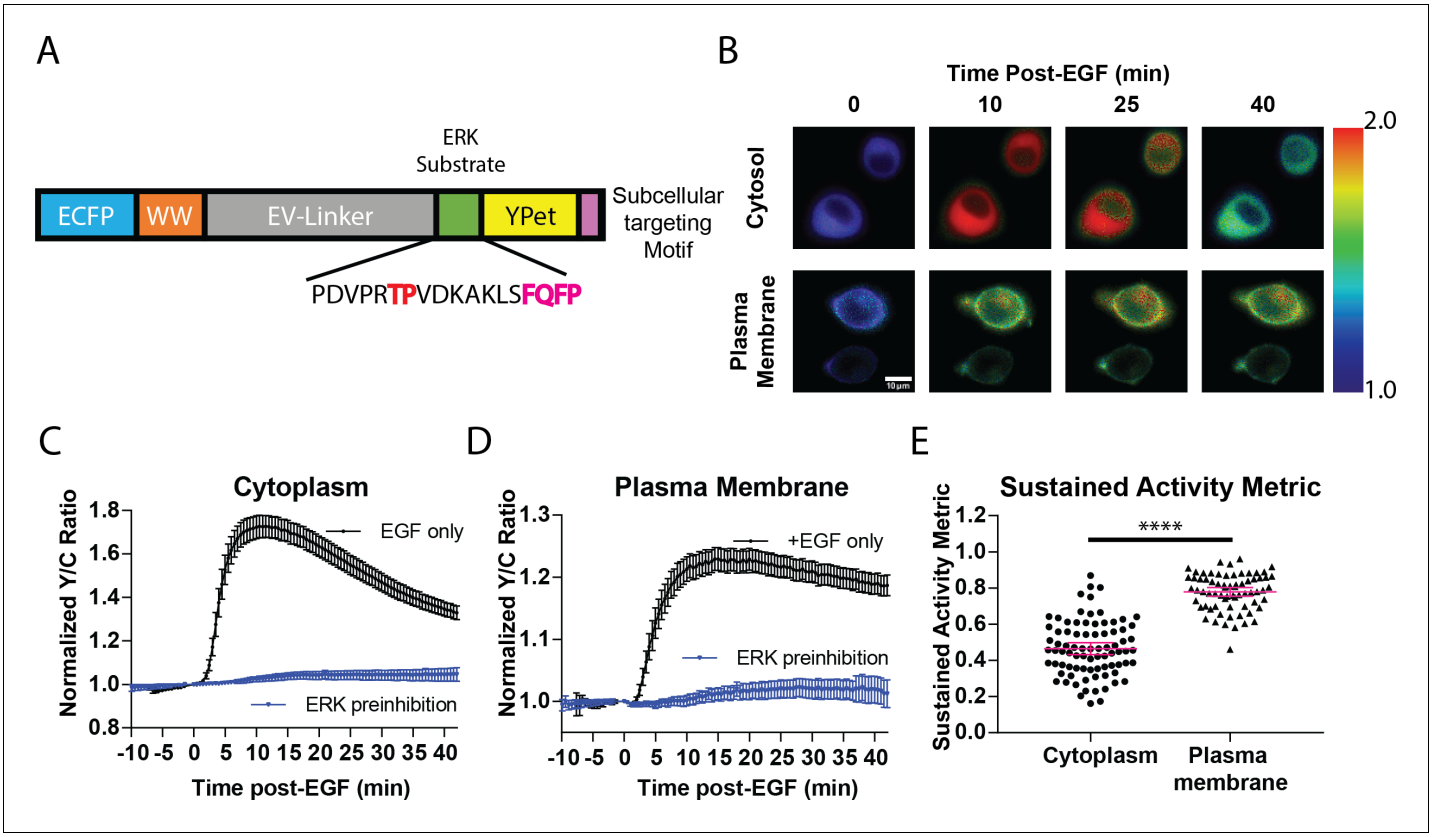

Figure 1. Targeted, FRET-based ERK biosensors reveal differential temporal dynamics of subcellular ERK activity. (**A**) Domain structure of improved ERK-kinase activity reporter (EKAR4). EKAR4 has two fluorescent proteins (ECFP and YPet) on N- and C-termini, respectively, with an ERK-specific substrate sequence, a phosphopeptide-binding domain (WW), and the EV-linker developed by ***Komatsu et al., 2011*** (**B**) Pseudocolor images representing the yellow over cyan (Y/C) emission ratio of cytosolic EKAR4 (cytoEKAR4) (top) versus plasma membrane-targeted EKAR4 (bottom) after EGF treatment at time 0. Warmer colors indicate higher Y/C emission ratio, scale bar = 10 μm. (**C**) Spatiotemporal dynamics of EGF-induced ERK activity in the cytosol. Cytoplasmic ERK activity was monitored using cytoEKAR4 in cells treated with 100 ng/μl EGF (black dotted line, n = 83) or pretreated with 10 μM SCH772984 (ERK inhibitor) 20 min before EGF (blue, triangles, n = 19). Each trace is a combined average of all cells. (**D**) Spatiotemporal dynamics of EGF-induced ERK activity at the plasma membrane. Plasma membrane localized ERK activity was monitored using the plasma membrane targeted EKAR4 (pmEKAR4) in cells treated with 100 ng/μl EGF (black dotted line, n = 71) or pretreated with 10 μM SCH772984 (ERK inhibitor) 20 min before EGF (blue, triangles, n = 24). Each trace is a combined average of all cells (see ***Figure 1—figure supplement 1A***, B for traces of all cells for C and D; Error bars represent 95% CI.) E) Activity persistence differences of ERK response to EGF between the cytoplasm and plasma membrane. Using the SAM40 metric (***Equation 1***), the transient versus sustained nature of ERK response to EGF at the cytoplasm (n = 83) and plasma membrane (n = 71) was quantified. (****p<0.0001 using one-way ANOVA multiple comparisons, see ***Figure 1—figure supplement 1D*** for comparison to nuclear ERK activity.) See also ***Figure 1—figure supplement 1***, ***Figure 1—figure supplement 2***.

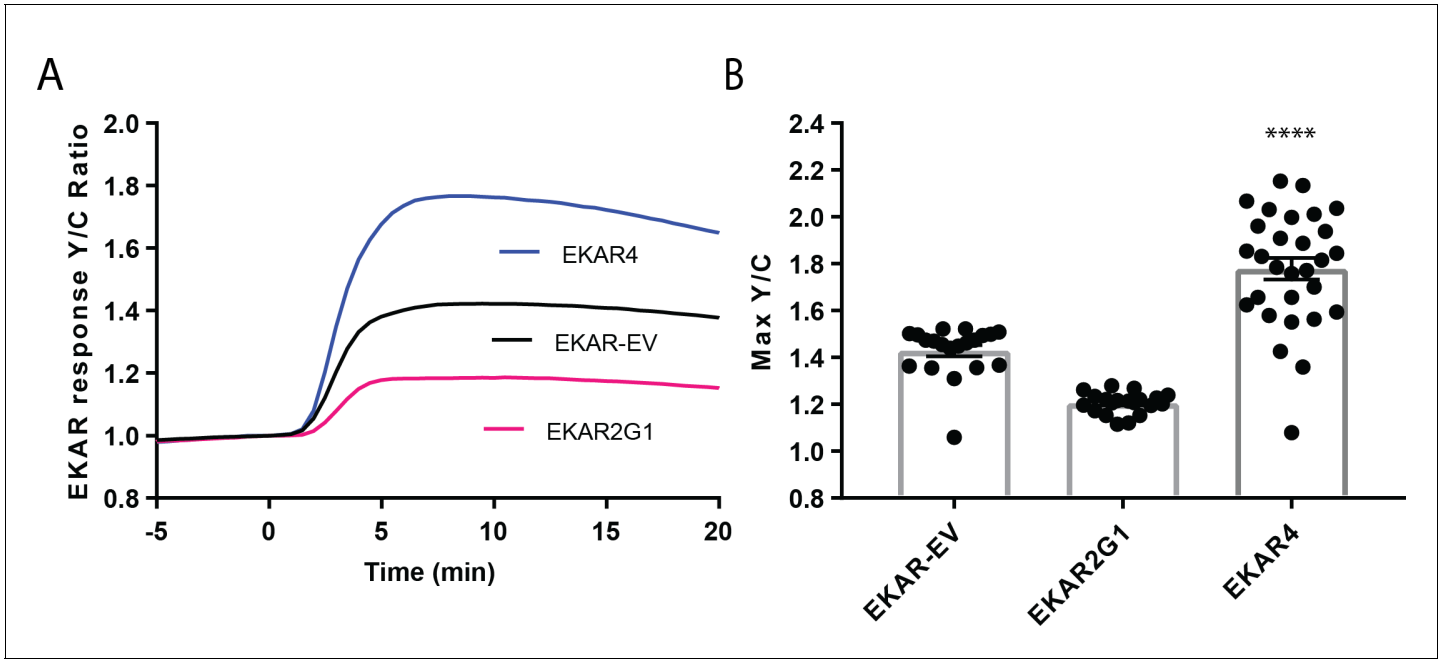

Figure 1—figure supplement 1. Direct comparison of EKAR4 to previous generations of EKAR in HEK-293T cells. (**A**) HEK-293T cells expressing either EKAR-EV (color, ref), EKAR2G1 (Color, ref), or EKAR4 (Color) were treated with 100 ng/ml EGF. Traces represent average activation curves from indicated replicates. (**B**) Amplitude of EGF-induced responses was compared between different EKARs. ($p<0.0001$).

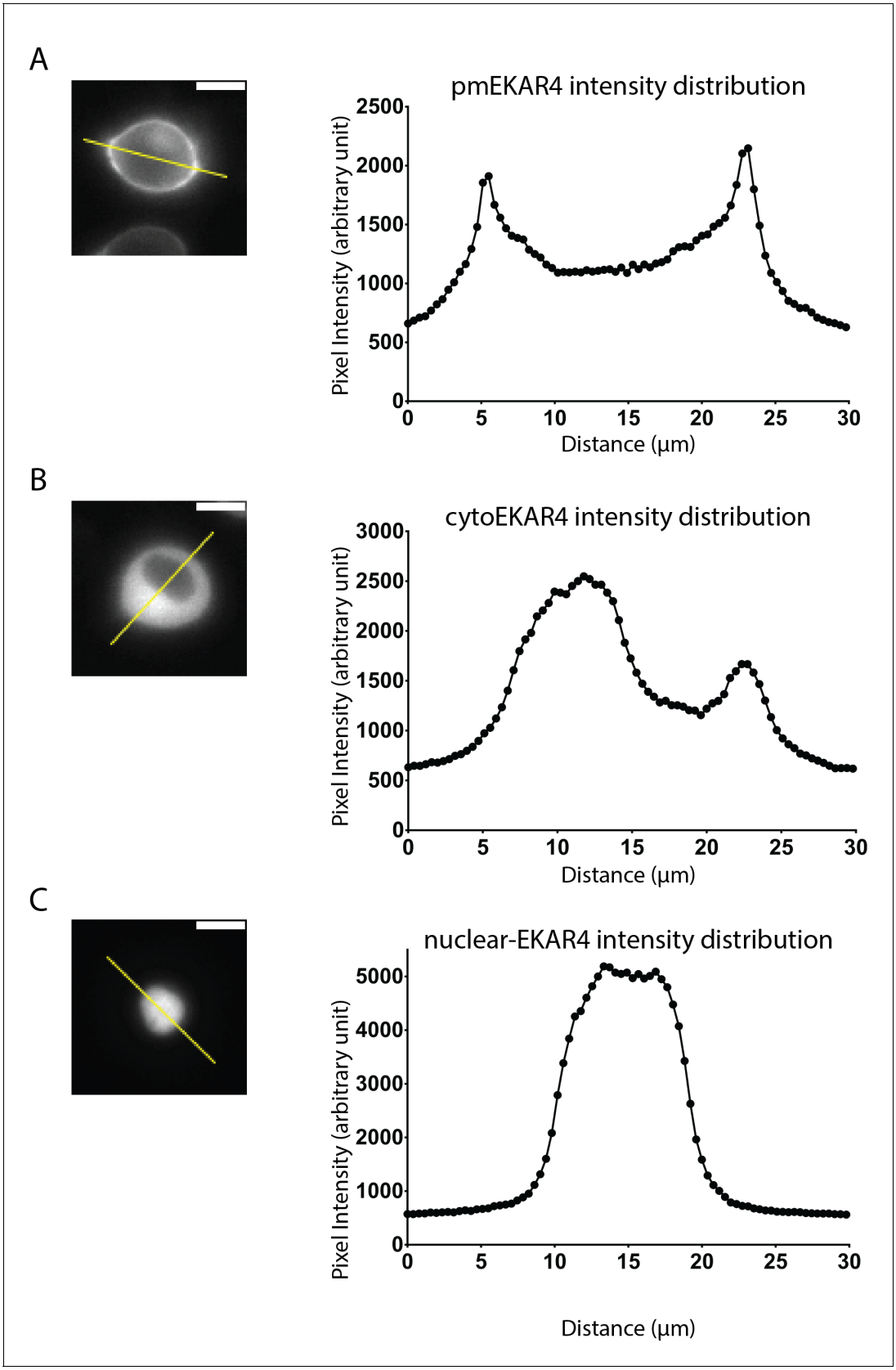

Figure 1—figure supplement 2. Verification of biosensor localization. Representative cells expressing either pmEKAR4 (**A**), cytoEKAR4 (**B**), or nuclear EKAR4 (**C**) were analyzed by measuring fluorescence intensity of the donor (ECFP) across the indicated line. Scale bar indicates 10 μm.

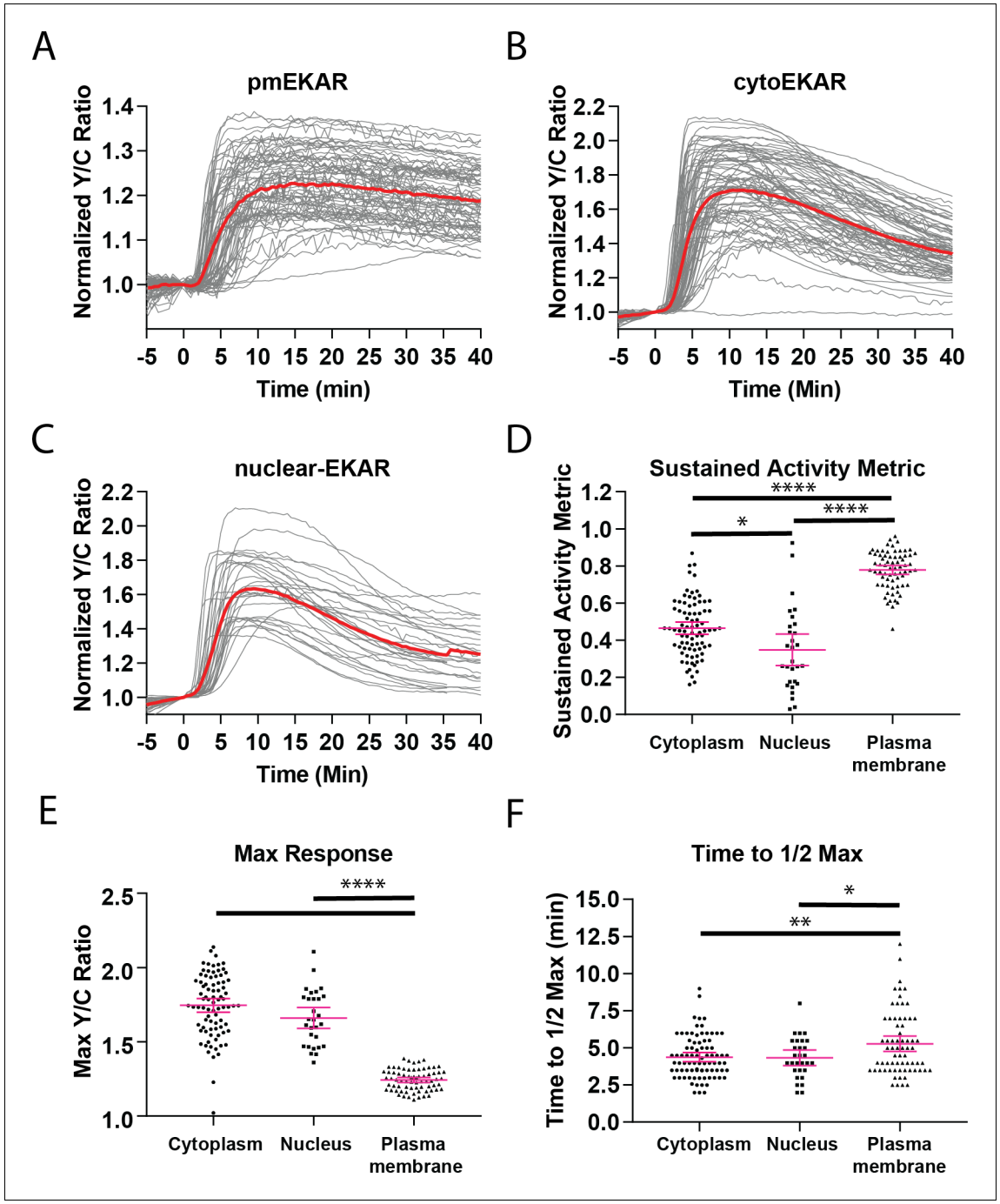

Figure 1—figure supplement 3. Single cell traces of EKAR responses reveal differential dynamics between subcellular locations. (**A**) All cell traces (n = 71) from plasma membrane targeted EKAR4 (pmEKAR4) in cells treated with EGF at time 0. Average shown in red. (**B**) All cell traces (n = 83) of cytosolic EKAR4 (cytoEKAR4) in cell treated with EGF at time 0. (**C**) All cell traces (n = 29) of nuclear-localized EKAR4 (nuclear EKAR4) in cells treated with EGF at time 0. (**D**) Sustained activity metric (SAM40) comparing cytoplasmic, nuclear, and plasma membrane EKAR responses. (**E**) Maximum FRET to donor emission ratio for each EKAR4. (**F**) EKAR4 response time comparisons between cytoplasmic, nuclear, and plasma membrane compartments. The time to ½ maximum responses was recorded and tabulated. Interestingly, cytoEKAR4 and nuclear EKAR4 respond before pmEKAR4, suggesting faster accumulation of ERK activity in cytosol which is dependent on both ERK and phosphatases. (Metric comparisons analyzed via one-way Anova with multiple comparisons, *p<0.05, **p<0.01, ****p<0.0001).

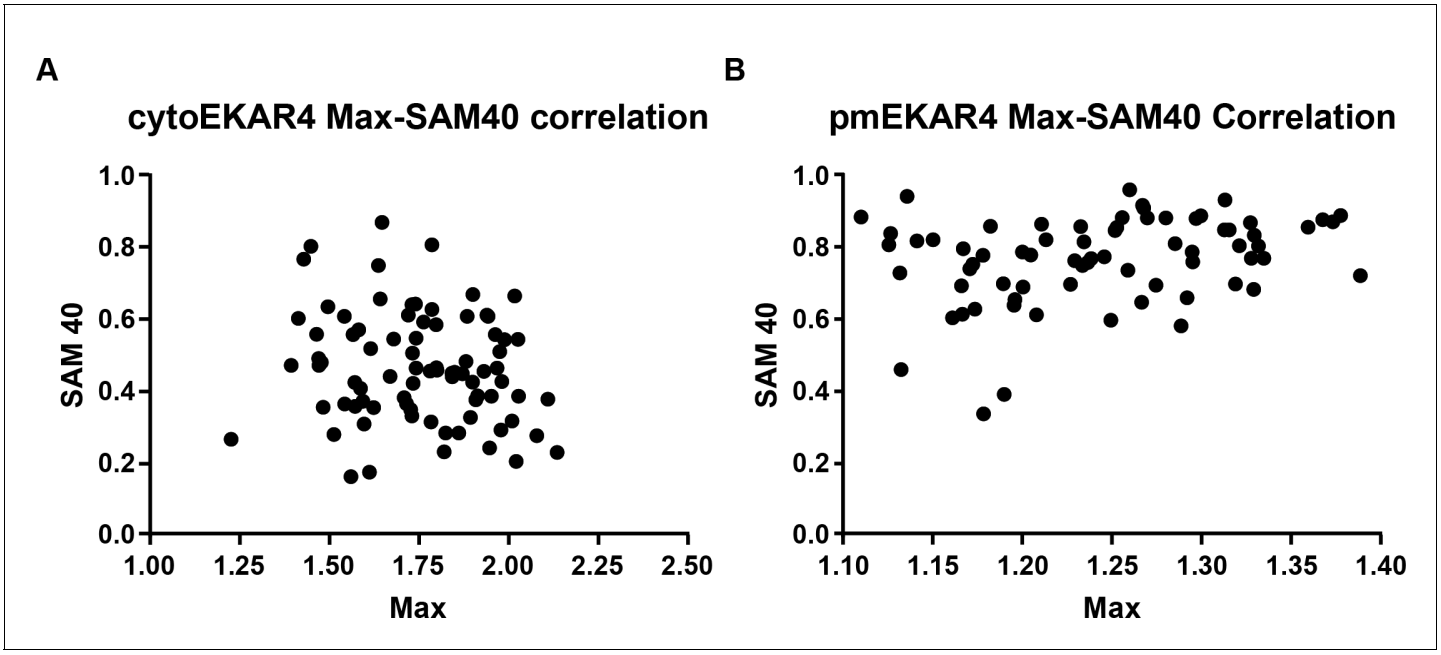

Figure 1—figure supplement 4. No significant correlation between EKAR4 signal amplitude and persistence. (**A**) Max Y/C Ratios plotted against SAM40 values for cytoEKAR4 (pearson's correlation coefficient 0.165). (**B**) Max Y/C Ratios plotted against SAM40 values for pmEKAR4 (pearson's correlation coefficient 0.2913).

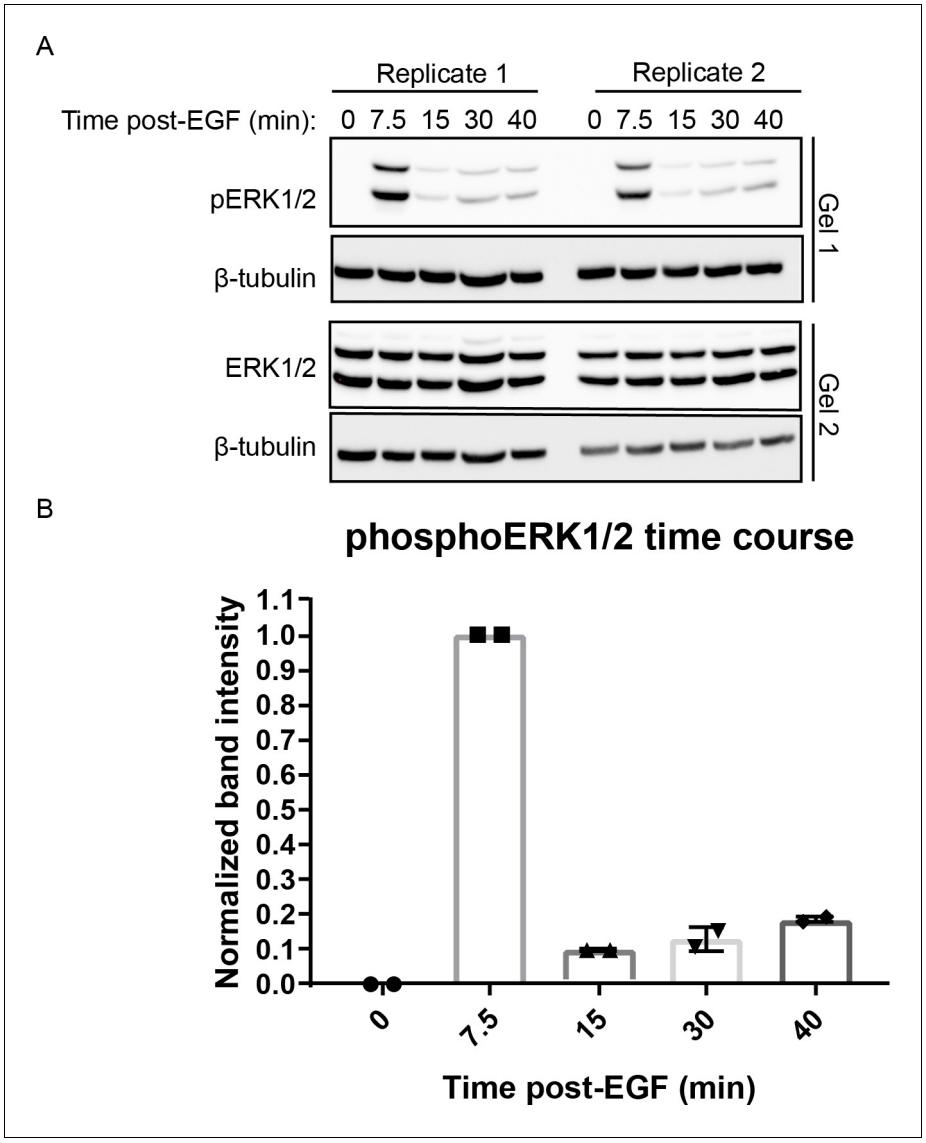

Figure 1—figure supplement 5. phoshpo-ERK time course. Cells were treated with 100 ng/mL EGF and harvested at indicated time points. Samples from each replicate were loaded on two separate gels and were subjected to western blot against both pERK1/2 (Gel 1) and total ERK1/2 (Gel 2) using β-Tubulin as loading control for each gel. Both ERK1/2 and pERK1/2 bands were normalized to associated β-tubulin loading control. After loading control normalization pERK1/2 was normalized total ERK signals, then the intensity at 7.5 min was set to 1 (n = 2 independent replicates).

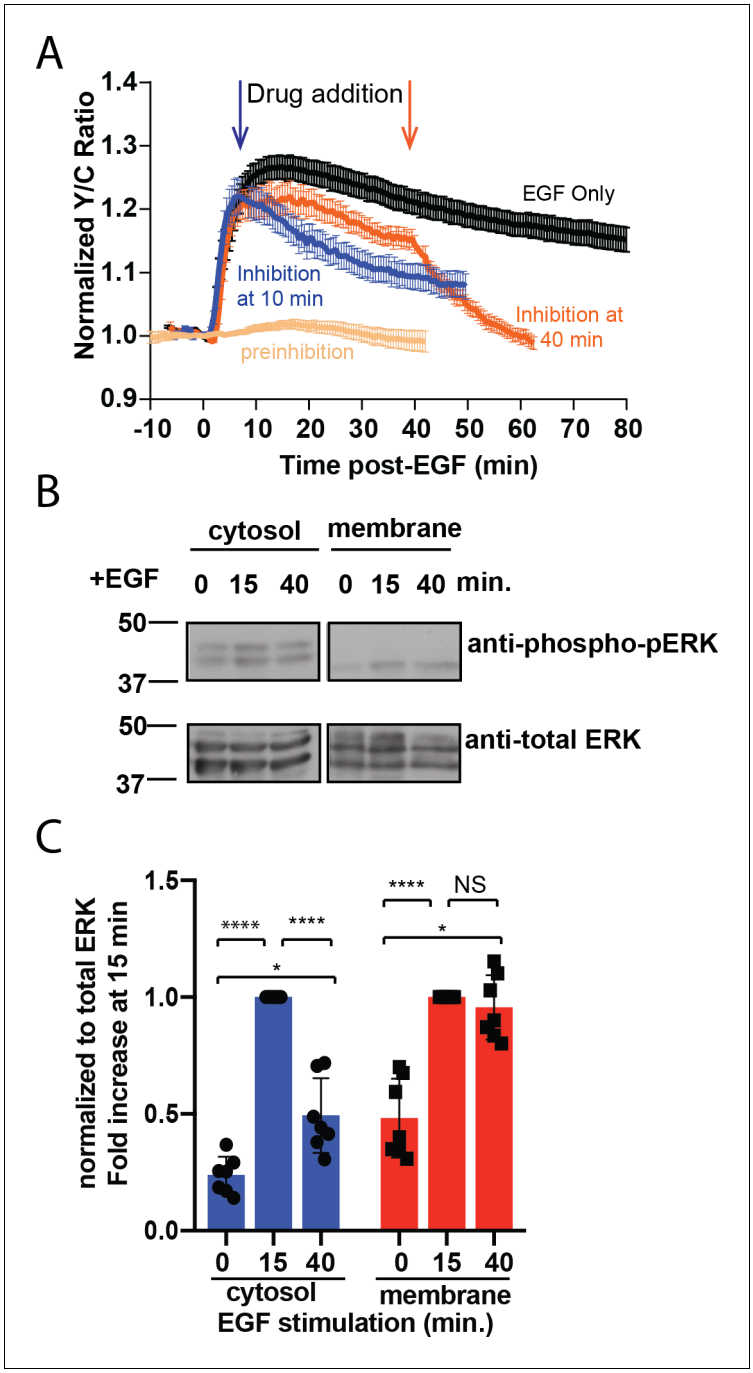

Figure 2. Sustained ERK activity at the plasma membrane is required for observed pmEKAR4 signal. (**A**) PC12 cells treated with the ERK inhibitor SCH772984 (10 μM) after EGF treatment at 10 min (n = 8) or 40 min (n = 8) post-EGF resulted in an immediate change in the slope of pmEKAR4 signal. (**B**) PC12 cells were harvested at select time points after EGF treatment and the lysates underwent subcellular fractionation, which is verified in ***Figure 2—figure supplement 1E***. After successful fractionation between the plasma membrane and other cellular components, a western blot against the phosphorylated and total form of ERK1/2 indicates that the levels of phospho-ERK remain relatively consistent up to 40 min after EGF treatment. Quantitation from five independent replicates is shown in panel C. (*p<0.05, ****p<0.0001, calculated using one-way ANOVA with multiple comparisons.) See also ***Figure 2—figure supplement 1***.

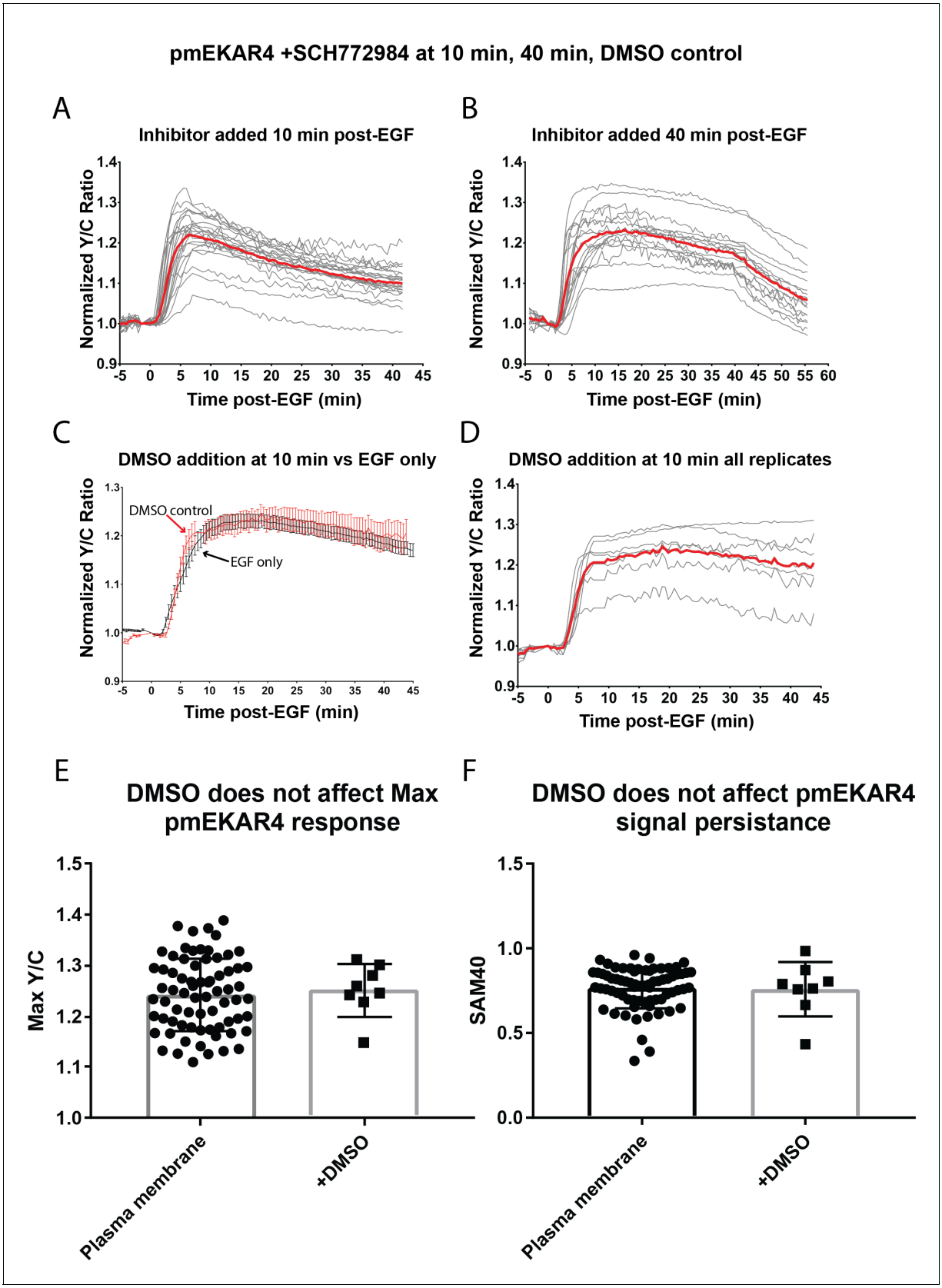

Figure 2—figure supplement 1. Responses of pmEKAR4 with ERK inhibitor treatment. (**A**) All Traces (n = 22) of pmEKAR in cells treated with 10 µM SCH772984 10 min after EGF. (**B**) All traces of pmEKAR in cells treated with 10 µM SCH772984 40 min after EGF addition (n = 17). (**C**) Average traces of

Figure 2—figure supplement 1 continued on next page

Figure 2—figure supplement 1 continued

EGF only (black trace) and DMSO-treated at 10 min post-EGF (blue trace) of pmEKAR response to EGF. (**D**) All pmEKAR traces of DMSO-treatment (n = 7). E. Verification that DMSO addition does not affect max pmEKAR response (p=0.75) F. Verification that DMSO does not affect pmEKAR4 signal persistence, as measured by the SAM40 metric (p=0.86).

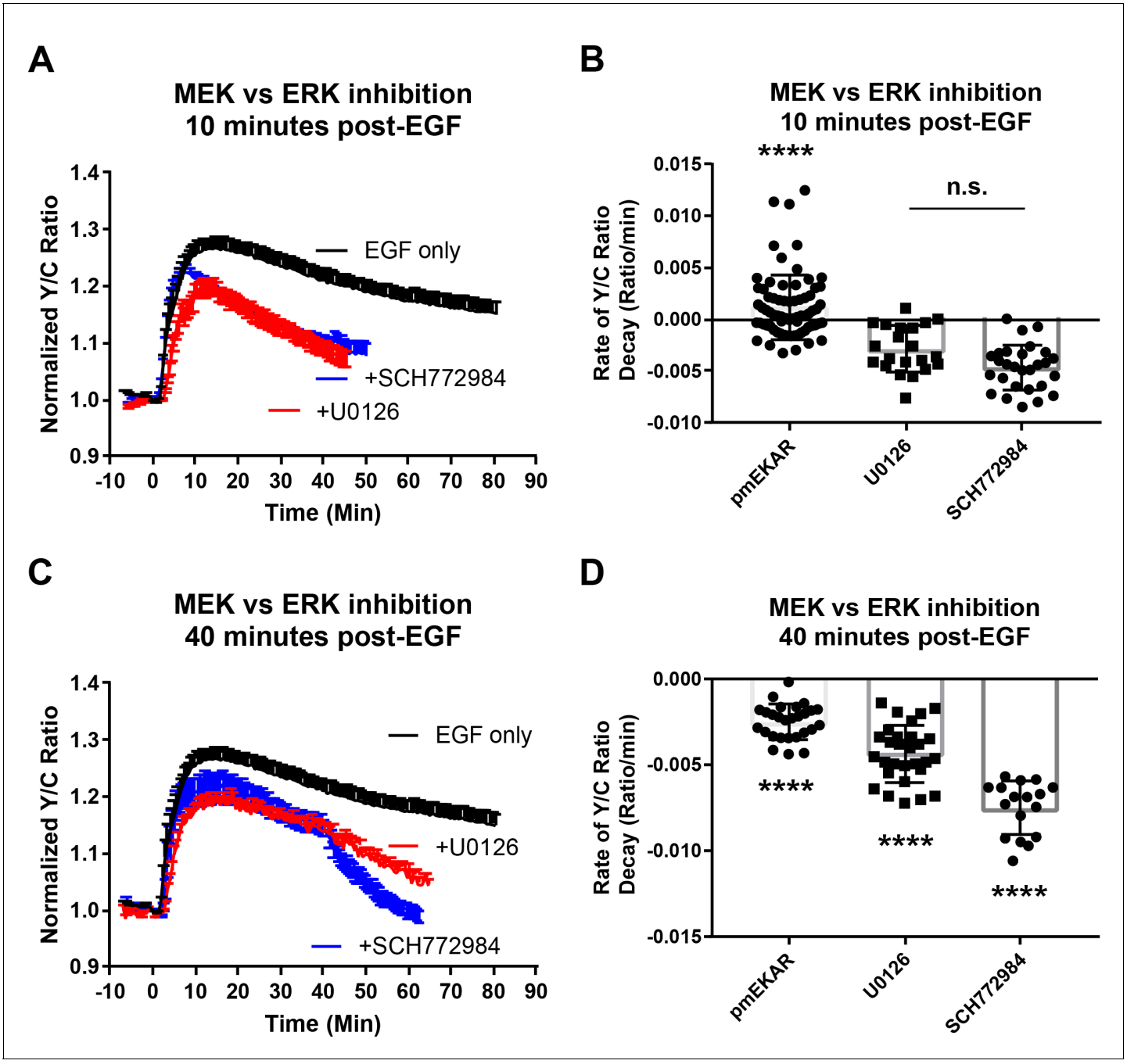

Figure 2—figure supplement 2. Reponses of pmEKAR4 with MEK inhibitor treatment. (**A–B**) Addition of 20 µM U0126 (MEK inhibitor) resulted in a decrease in slope of decay of pmEKAR4 signal (****p<0.0001 compared to both U0126 (n = 21) and SCH772984 (n = 28)). (**C–D**) Addition of 20 µM U0126 (n = 29) at 40 min post EGF also led to a decrease in the slope of pmEKAR4 signal, indicating MEK was active (p<0.0001 with Ordinary one-way Anova with multiple Comparisons – each condition compared to every other condition.).

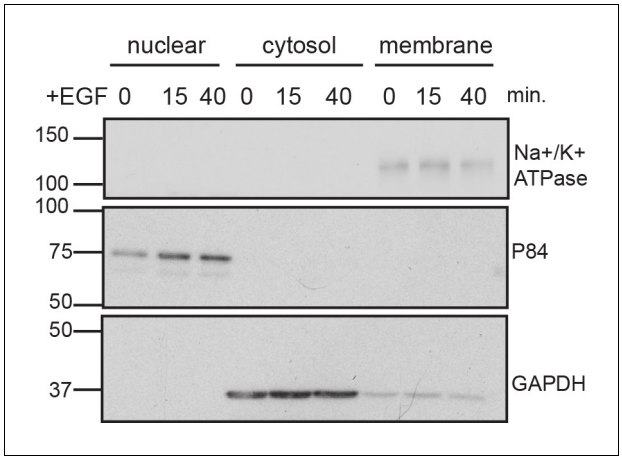

Figure 2—figure supplement 3. Verification of successful subcellular fractionation. PC12 cells treated with EGF at indicated time points were harvested and subjected to subcellular fractionation and immunoblot as described in Materials and methods.

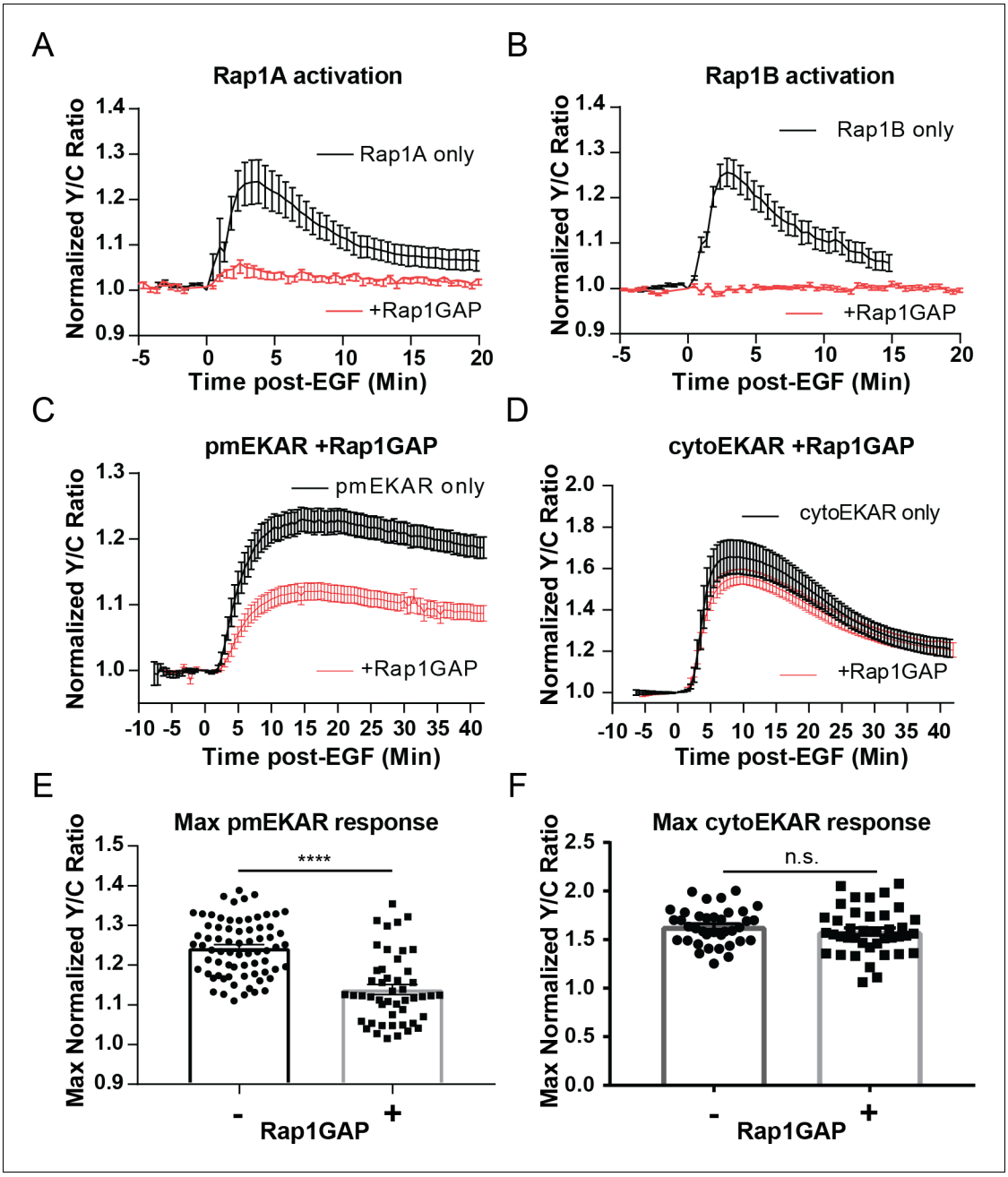

Figure 3. Rap1 GTPase regulates EGF-induced ERK activity at the plasma membrane. Cells expressing either (**A**) diffusible Rap1A FLARE (n = 11) or (**B**) diffusible Rap1B FLARE (n = 9) were treated with EGF at time 0, increase in yellow over cyan (Y/C) emission ratio indicates Rap1 activation. The observed increases in ratio are abrogated by co-expression of the Rap1-specific GAP Rap1GAP (red curves, n = 14, n = 15, respectively). (**C, E**) Rap1GAP expression significantly dampened pmEKAR4 response (n = 40). (**D, F**) Rap1GAP expression had no significant effect on cytosolic ERK activity (n = 40). (****p<0.0001, n.s. = not significant, calculated using student's t-test with Welch's correction) See also ***Figure 3—figure supplements 1–6***.

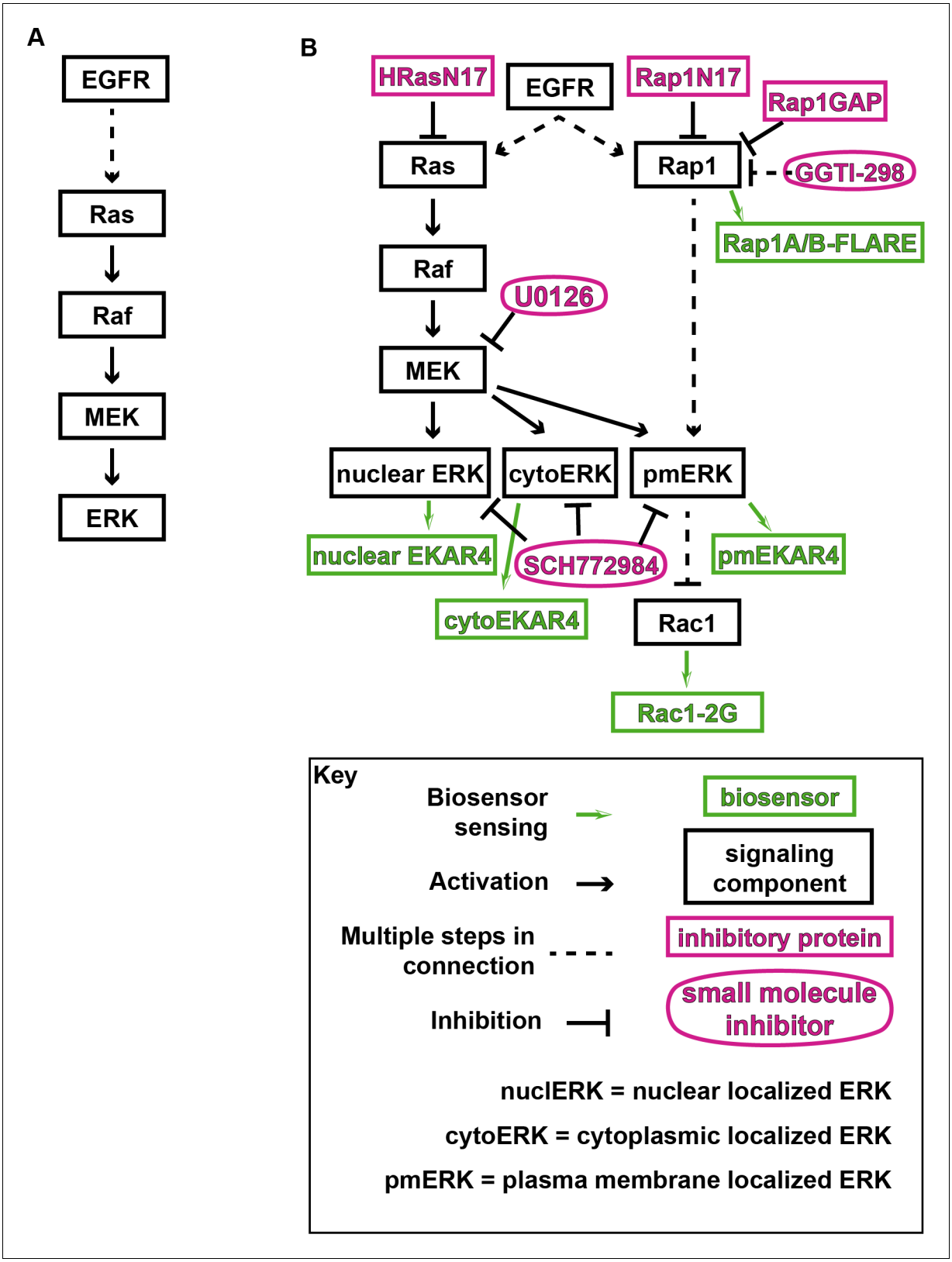

Figure 3—figure supplement 1. Model of ERK and tested pathways. (**A**) Canonical ERK/MAPK signaling pathway. (**B**) EGFR signaling pathway components with inhibitors and biosensors used in this study.

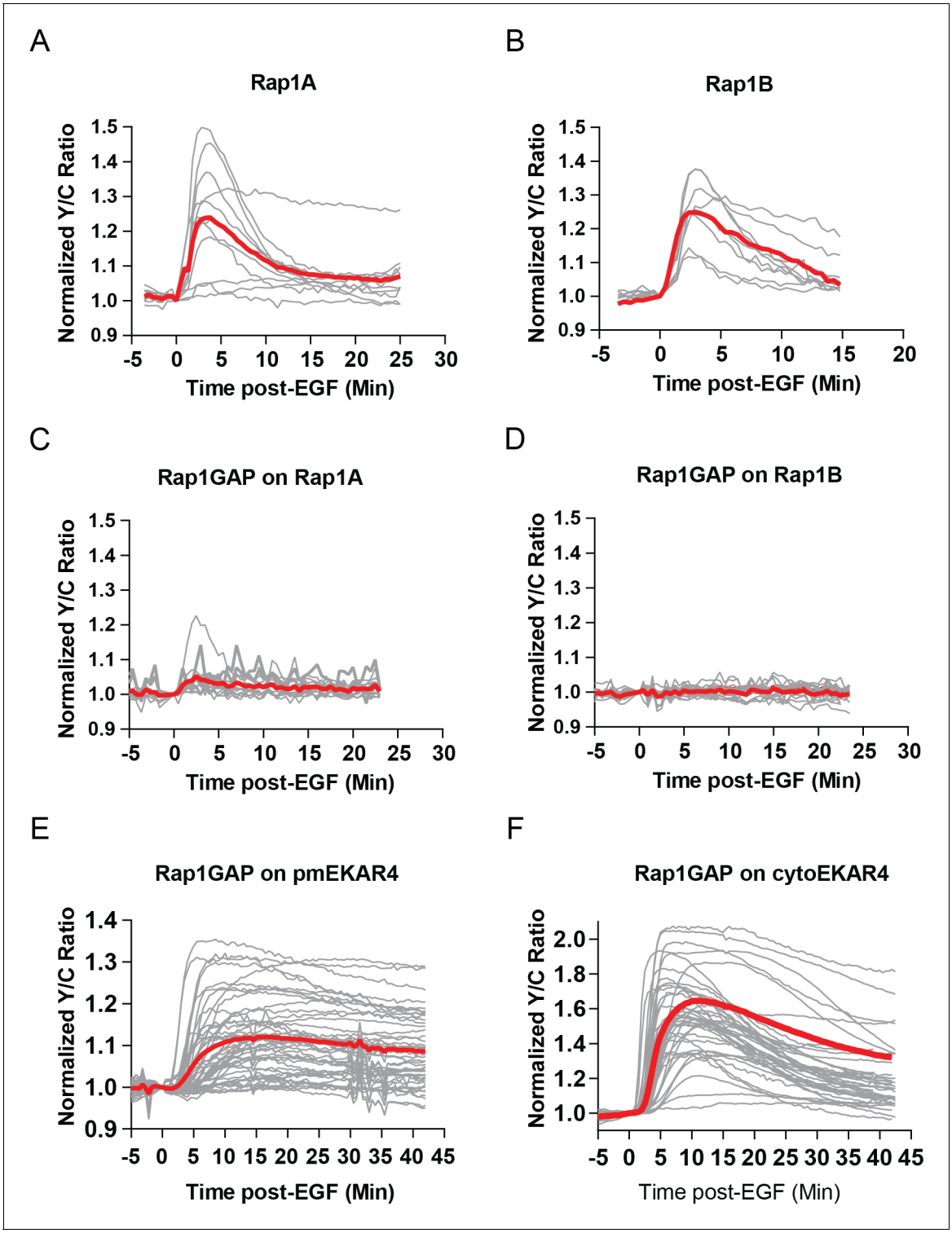

Figure 3—figure supplement 2. Rap1-FLARE responses of all replicates. (**A**) Rap1A FLARE responses of all replicates, average shown in red (n = 11). (**B**) Rap1B FLARE responses of all replicates with average shown in red (n = 9). (**C**) Effect of Rap1GAP expression on Rap1A FLARE response, all replicates (n = 14). (**D**) Effect of Rap1GAP on Rap1B Flare response, all replicates (n = 15). (**E**) Effect of Rap1GAP on pmEKAR4 responses, all replicates (n = 40). (**F**) Effect of Rap1GAP on cytoEKAR4 responses, all replicates (n = 40).

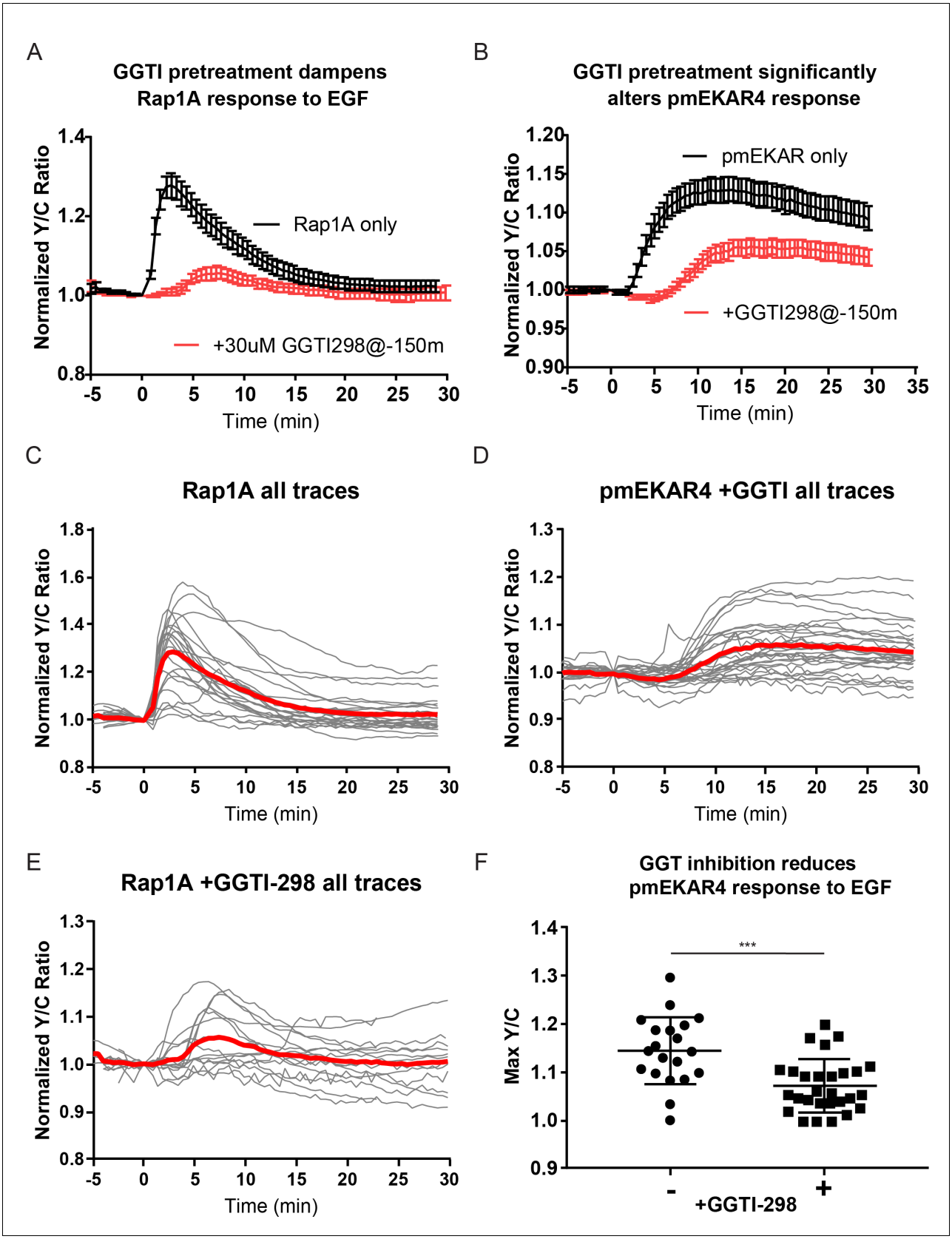

Figure 3—figure supplement 3. Abrogation of Rap1 signaling via geranylgeranyl transferase inhibition significantly dampens plasma membrane ERK response. (**A**) 30 µM GGTI-298 addition to cells 150 min before EGF treatment led to a drastic decrease in the Rap1A response to EGF. (n = 24 GGTI

Figure 3—figure supplement 3 continued on next page

Figure 3—figure supplement 3 continued

control; n = 15 +GGTI) B) 30 μM GGTI-298 addition to cells 150 min before EGF dampens pmEKAR4 response to EGF (n = 20 GGTI control; n = 28 +GGTI control.) C-E) individual traces of all replicates for indicated conditions, red curve represents average.) F) Quantitation of max amplitude of pmEKAR4 response with and without GGTI-298 preincubation. (***p=0.0002, unpaired t-test).

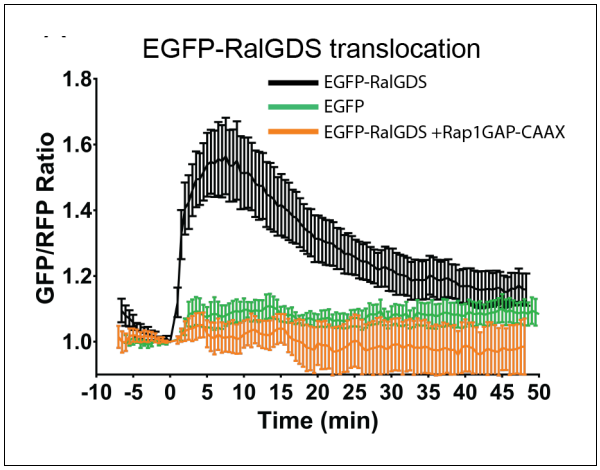

Figure 3—figure supplement 4. Ral-GDS translocation assay reveals EGF-mediated activation of Rap1 at the plasma membrane. Cells expressing either a plasma membrane targeted mCherry-CAAX (mCh) in combination with either EGFP-RalGDS (black curve, n = 11 cells), EGFP only (green curve, n = 3 cells), or EGFP-RalGDS with Rap1GAP overexpression (orange curve, n = 5 cells) were analyzed using TIRF microscopy to track EGFP translocation to the basal membrane, indicating the formation of GTP-bound Rap1 at the plasma membrane.

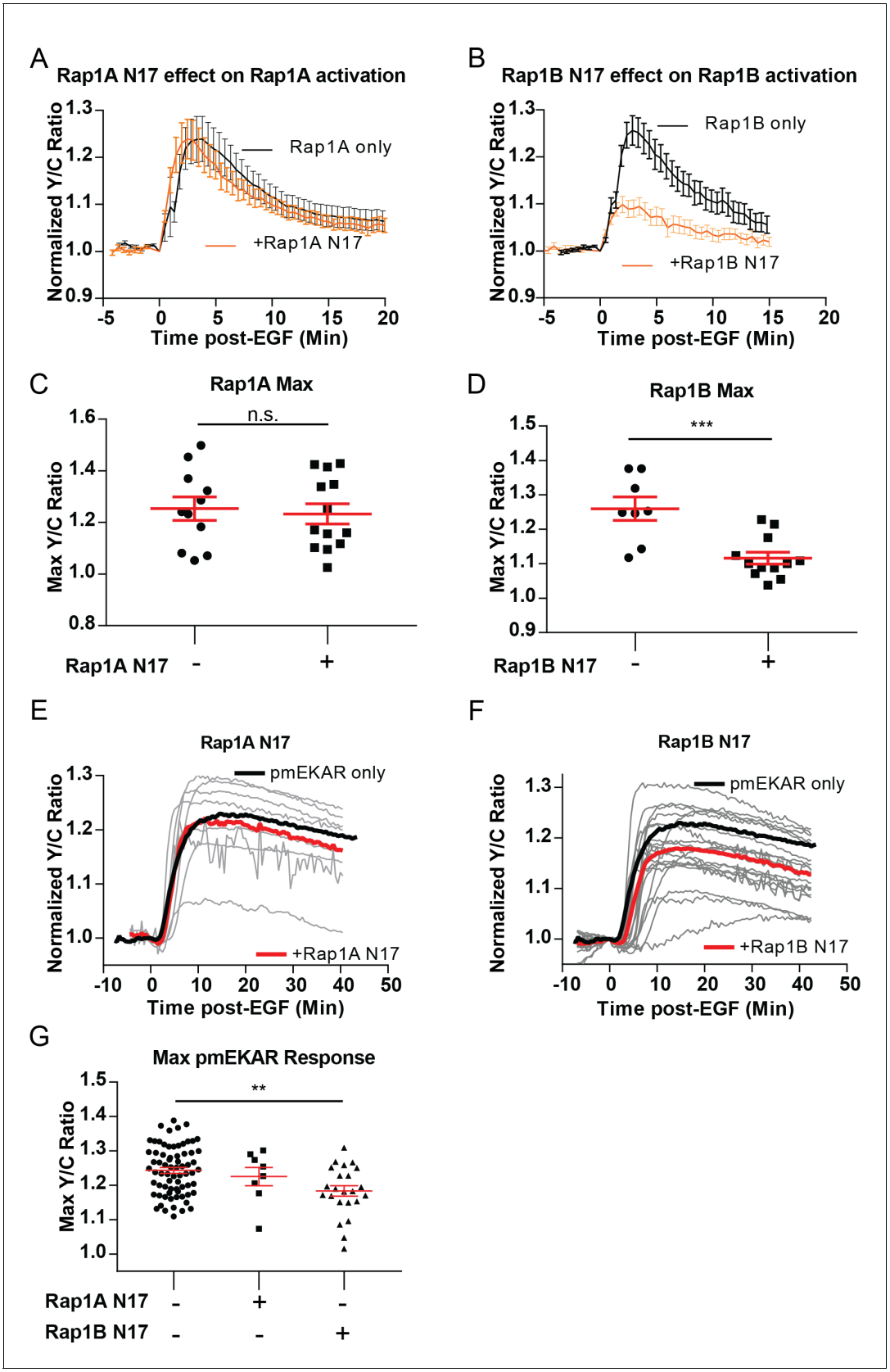

Figure 3—figure supplement 5. Dominant negative Rap1 isoforms on EGF-induced Rap1 and plasma membrane ERK responses. Rap1A N17 expression had no effect on Rap1A FLARE response (**A, C**) or pmEKAR response to EGF (**E, G**). Rap1B N17 expression significantly dampened Rap1B

Figure 3—figure supplement 5 continued on next page

Figure 3—figure supplement 5 continued

response (**B, D**) and dampened pmEKAR4 response (**F, G**) (n = 23). Note, Rap1 DN expression resulted in similar trends as Rap1GAP expression, but the effect had more cell-to-cell variability. (***p<0.001, student's t-test; **p<0.01, one-way Anova comparison to no dominant negative control).

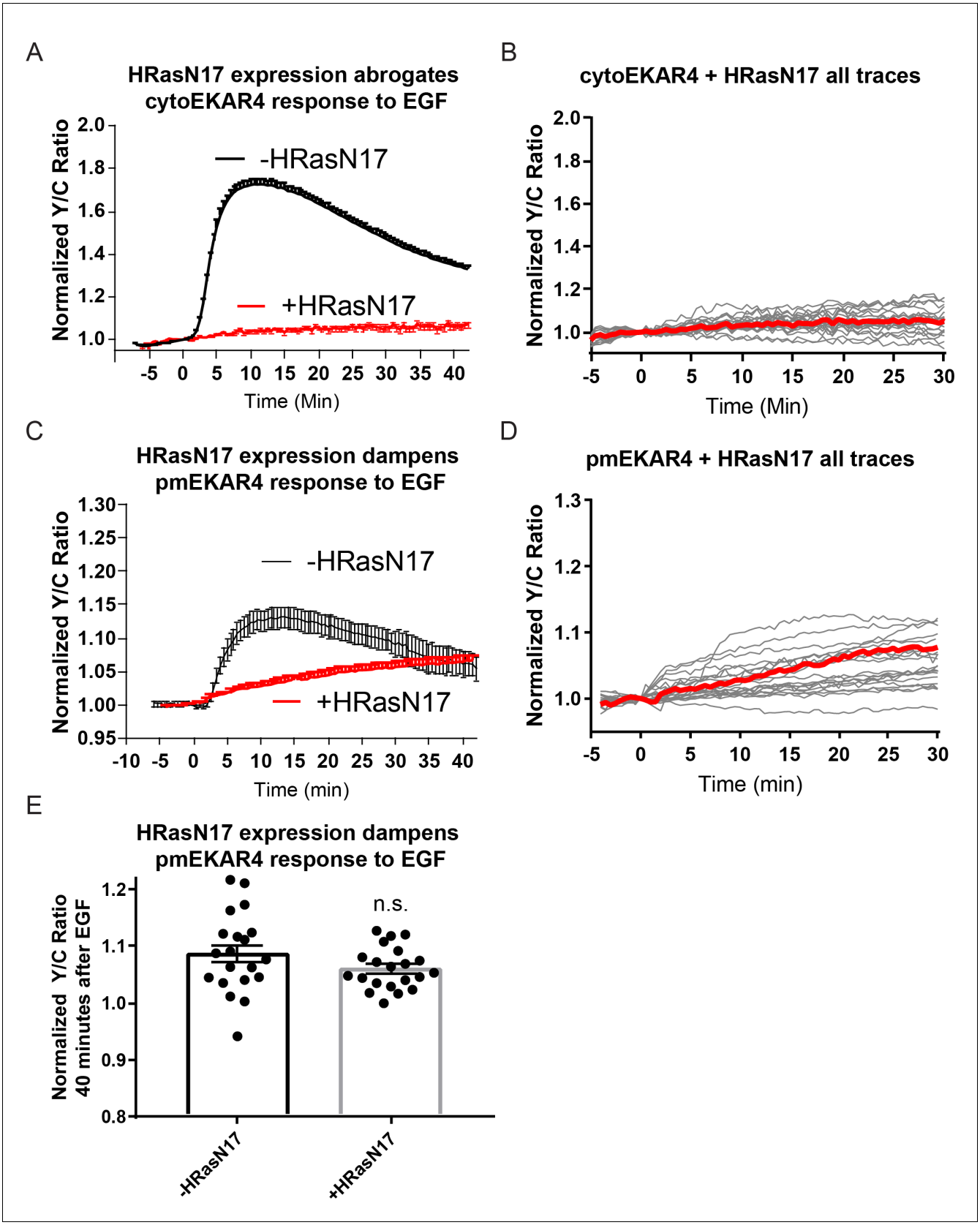
A
HRasN17 expression abrogates cytoEKAR4 response to EGF
Normalized Y/C Ratio
-HRasN17
+HRasN17
Time (Min)
B
cytoEKAR4 + HRasN17 all traces
Normalized Y/C Ratio
Time (Min)
C
HRasN17 expression dampens pmEKAR4 response to EGF
Normalized Y/C Ratio
-HRasN17
+HRasN17
Time (min)
D
pmEKAR4 + HRasN17 all traces
Normalized Y/C Ratio
Time (min)
E
HRasN17 expression dampens pmEKAR4 response to EGF
Normalized Y/C Ratio 40 minutes after EGF
n.s.
-HRasN17
+HRasN17

Figure 3—figure supplement 6. Effect of HRasN17 dominant negative expression on cytoEKAR4 and pmEKAR4 response to EGF in PC-12 cells. (**A–B**) HRasN17 expression completely abrogates cytosolic ERK response (n = 21). (**C–D**) Plasma membrane localized ERK exhibits a dampened, slow response to EGF (n = 21). (**E**) Quantification of average amplitude value at 40 min post EGF. (n.s. = not significant).

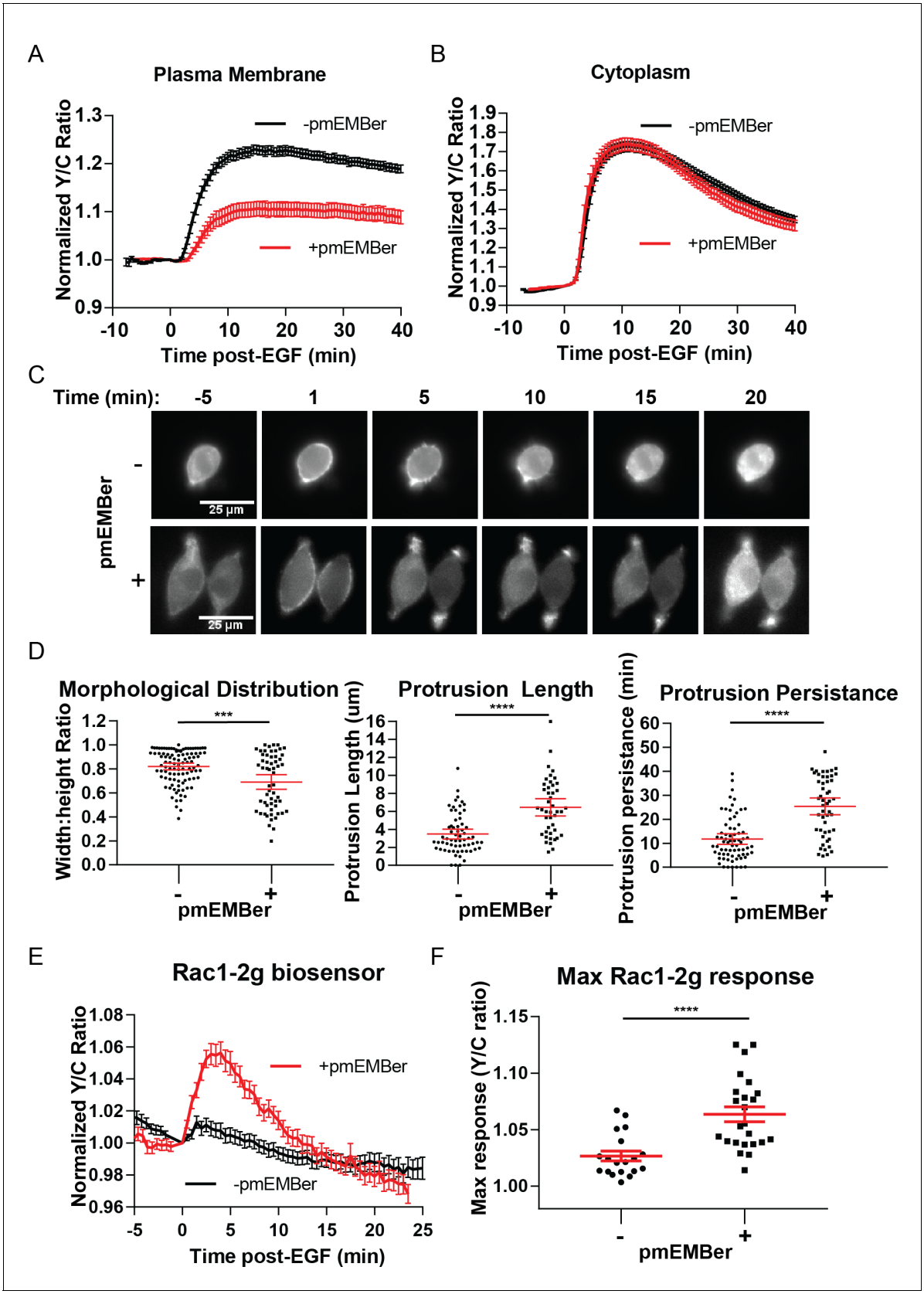

Figure 4. Inhibition of plasma membrane localized ERK activity alters cell morphology, EGF-induced protrusions, and Rac1 activation. (**A**) Effect on pmEKAR4 response to EGF in PC12 cells expressing a plasma membrane-targeted monobody EMBer7.1 (pmEMBer) (***Mann et al., 2013***) which binds

Figure 4 continued on next page

Figure 4 continued

to ERK and dampens ERK activity (n = 36 cells, red curve). (**B**) Effect on cytoEKAR4 response to EGF in PC12 cells expressing pmEMBer (n = 37 cells, red curve) (**C**) Representative images of cell morphology and protrusion dynamics in response to EGF in PC12 cells with (bottom row) or without (top row) pmEMBer expression. (**D**) (Left-most panel) Major and minor axes of each cell was measured using ImageJ and the ratio of minor: major was calculated for each cell with and without pmEMBer expression. Kymographs generated from major axes of each cell plotting distance and time (***Figure 4—figure supplement 2***) were used to quantitate protrusion length in μm and protrusion persistence in min. (Middle and right panels) (n = 103 pmEMBer, n = 57 +pmEMBer, ***p=0.0002, ****p<0.0001) (**E**) Using Rac1-2G biosensor to measure Rac1 activity (***O'Shaughnessy et al., 2019***), cells either expressing pmEMBer (red curve, n = 24 cells) or pm-mCherry (black curve, n = 19 cells) were treated with EGF. (**F**) Quantitation of Max Rac1-2G response to EGF. (p<0.0001, Welch's t-test to correct for different variances.) See also ***Figure 4—figure supplement 1***, ***Figure 4—figure supplement 2***, ***Figure 4—figure supplement 3***.

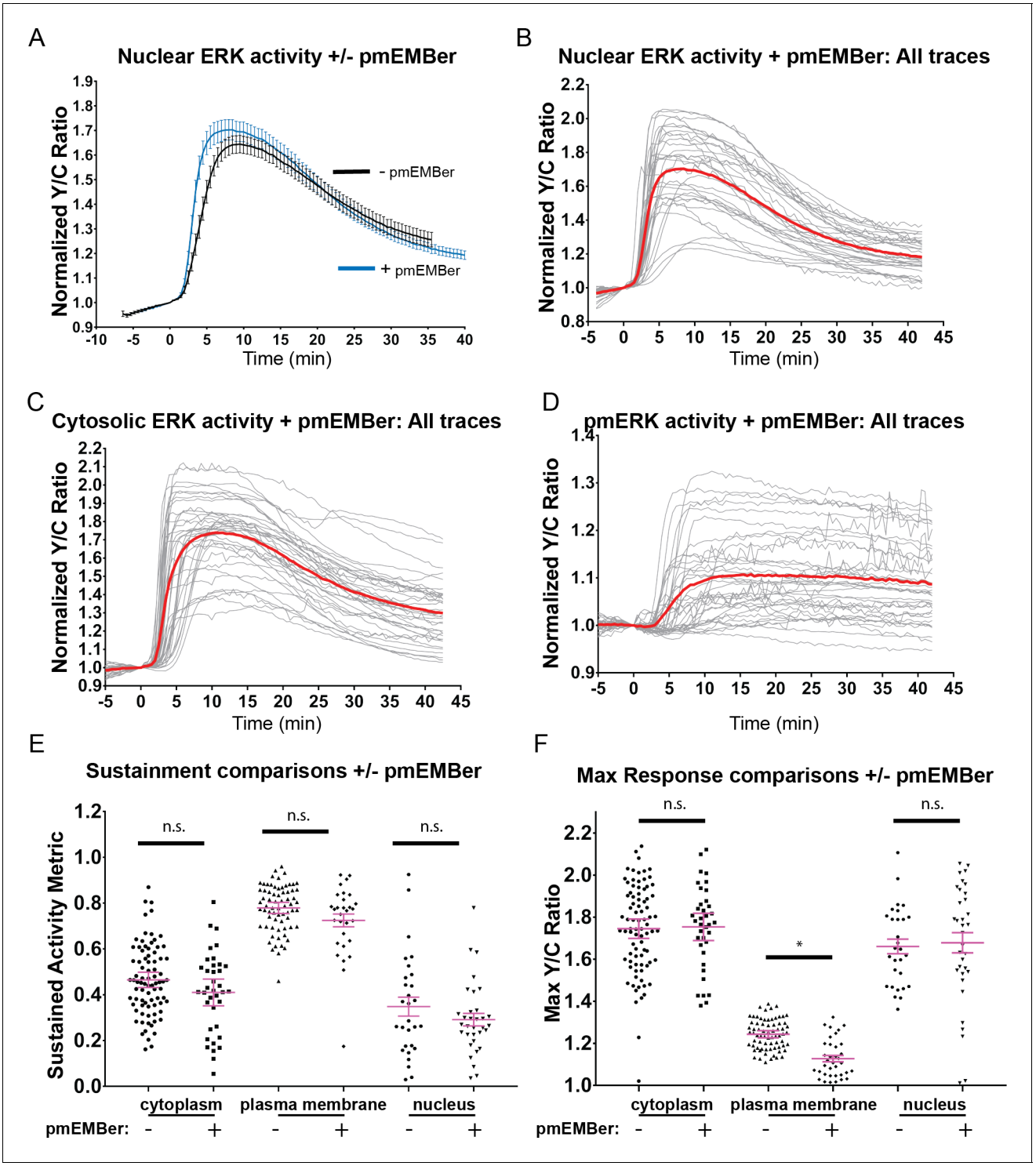

Figure 4—figure supplement 1. Effects of pmEMBer on ERK and PC-12 responses to EGF. (**A**) Effect of pmEMBer expression on nuclear ERK response to EGF. (**B**) All traces of nuclear ERK responses in EGF stimulated cells expressing pmEMBer (n = 32). (**C**) All traces of cytoplasmic ERK responses in EGF-stimulated cells expressing pmEMBer (n = 75). (**D**) All traces of plasma membrane ERK responses in EGF-stimulated cells expressing pmEMBer (n = 36). (**E**) Effect of pmEMBer expression on sustainment of ERK responses, measured by SAM40 metric (***Equation 1***). Each condition was compared to every other condition using one-way ANOVA with multiple comparisons. Each location (plasma membrane, cytoplasm nucleus) showed no significant change in persistence of ERK activity. (**F**) Effect of pmEMBer on maximum response (Y/C ratio) at the cytoplasm, plasma membrane, and nucleus. Each condition was compared to every other condition using one-way ANOVA with multiple comparisons. (n.s. = not significant, *p<0.05.).

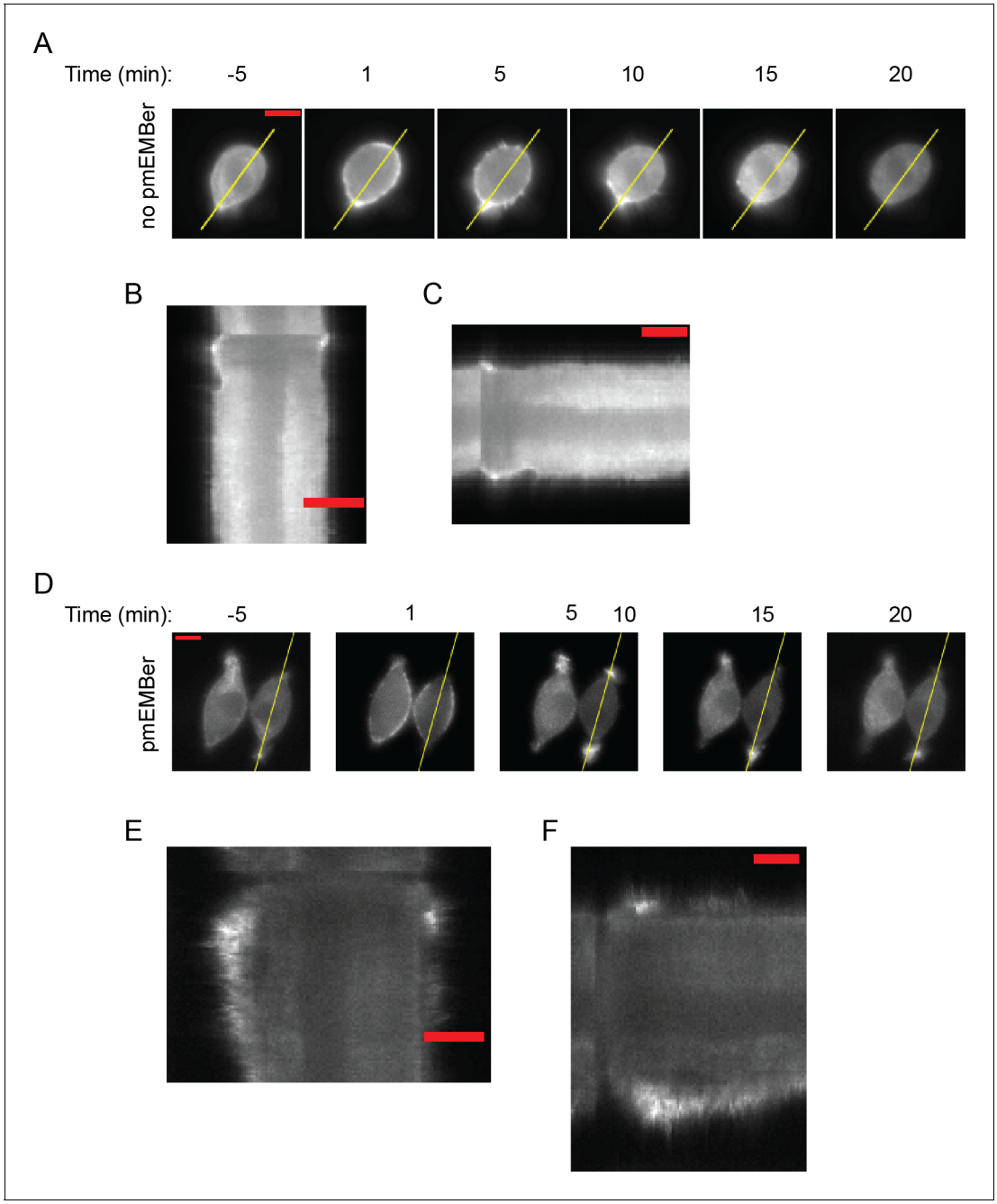

Figure 4—figure supplement 2. Examples of cell protrusion measurements. (**A, D**) Kymograph of indicated area in was obtained along the major axis to quantitate cell protrusions. (**B, E**) Kymographs of cell shown in (**A**) and (**D**), respectively. Scale bar represents 10 µm. (**C, F**) Kymographs from (B or E) were rotated so that the horizontal axis represents time. Scale bar represents 600 s (10 min.).

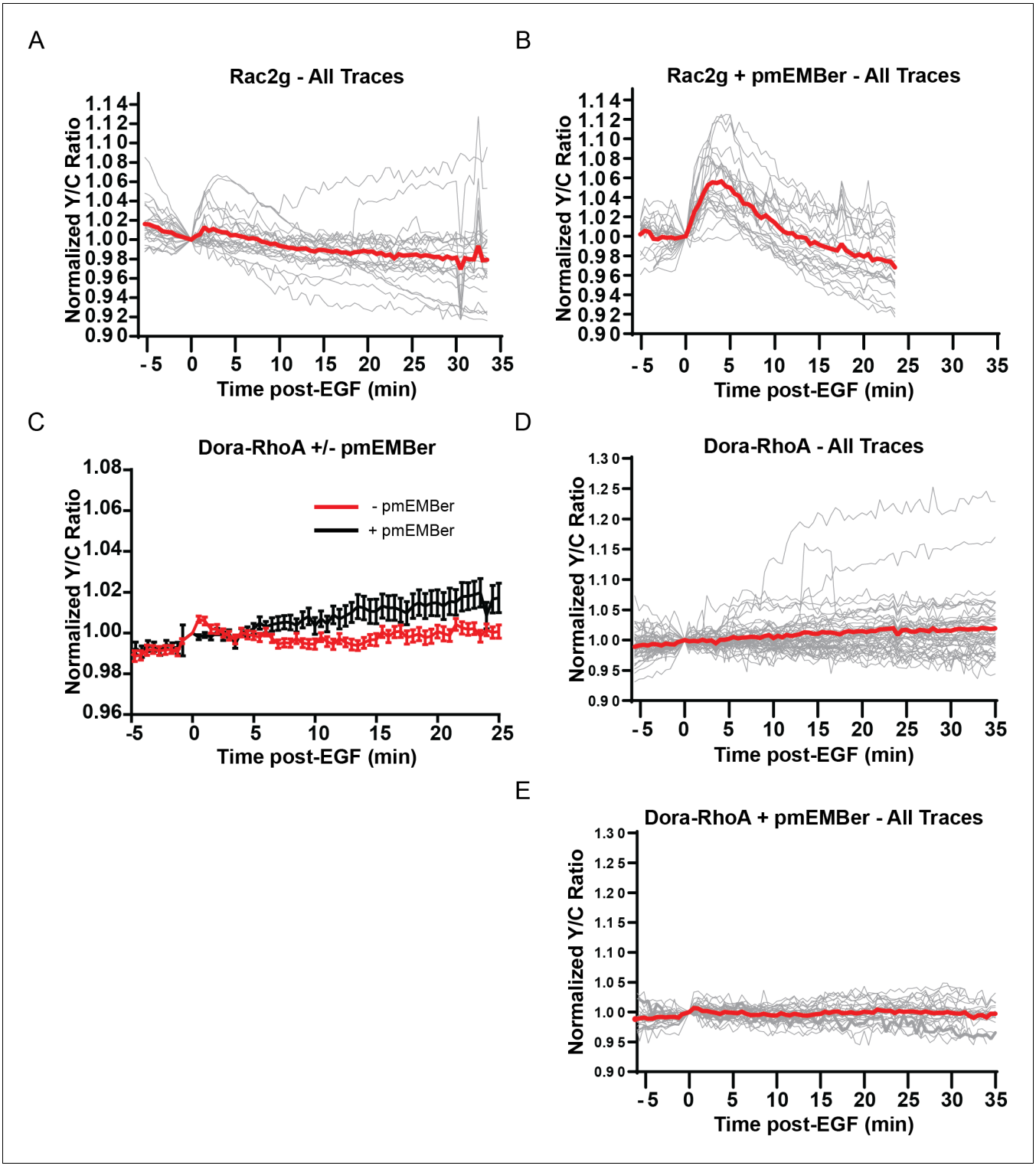

Figure 4—figure supplement 3. Effect of pmEMBer on Rac1 and RhoA responses to EGF in PC12 cells. (**A**) All traces (n = 19) of the effect of EGF on Rac1 measured by the Rac-2G biosensor. Average displayed as red trace. (**B**) All Traces of Rac1 activity in presence of pmEMBer, n = 24. (**C**) Average traces comparing RhoA activation in response to EGF with or without pmEMBer expression. (**D**) All traces of RhoA activation in cells expressing mCh-CAAX control (n = 50). (**E**) All traces of RhoA activation in cells expressing pmEMBer (n = 30).